



Sudan University of science & Tecnology
College of petroleum Engineering & Technology
Departed of Petroleum Engineering



Identification of petrophiscal reservoir water saturation properties using the comparison of capillary model and log model

تحديد خصائص تشبع المياه المكامن البتروفيزيائية وذلك سجلات الآبار مقارنة النماذج الشعيرية ونماذج باستخدام

Presented by:

Othman Abdullah Ahmed Al- Qaisi

Abdelmula Adam Salih

Adam Hassan Mahmoud Al – Roum

Mohammed Mahmoud Mohammed Al - Shekh

Supervised by:

Dr. Alradi Abbas

October-2017

قال تعالى:

((وَقُلْ رَبِّ زِدْنِي عِلْمًا)) سورة طه آية 114

Dedication

For those who have been teaching me that the things which go wrong are often the very things that lead to other things going right, for whom encourage me to be brave enough to live life creatively Mom & Dad , the least I can do is to dedicate my project to you.

This dedication extends to include my inspiration source Reham who was and still is illuminating my dark in my worst cases.

For my future's sons (Odai and Madleen) this project will be dedicated to you as well because I want you to know that the future holds adventures in every day, opportunities in every challenge and possibilities in every dream.

A huge thanks and appreciation for my sisters, brothers and friends who were supporting me all the time.

Eng. Othman Abdullah AL-Qaisi

For their countless sleepless night filled with prayers and hopes for our success in life, the least we could do is to dedicate our efforts to the three most influential people in my life dad, mam, sisters and brothers.

The dedication extended to my wife and kids.

Eng. Abdelmula Adam Salih

To mother and father whom we bare this success and never slept in night to see us on the top.

To our doctors and lecturers that helped us through our studies and spent a lot of their times to supply us with knowledge and worked hard to graduate us.

To my brothers, sisters and family class mates.

To everyone who helped me without forgetting someone.

Eng. Mohammed Mahmoud Mohammed Al-Shekh

لابد لنا ونحن نخطوا خطواتنا الأخيرة في الحياة الجامعية، من وقفة نعود إلى أعوام قضيناها في رحاب الجامعة، مع أساتذتنا الكرام الذين قدموا لنا الكثير، باذلين بذلك جهودا كبيرة في بناء جيل الغد؛ لِتُبَعَثَ الأمة من جديد ...

وإلى رمز الرجولة والتضحية، إلى سندي وقوتي وملاذي بعد الله، إلى من كلله الله بالهيبة والوقار، إلى من علمني العطاء بدون انتظار، إلى من أحمل أسمه بكل افتخار، أرجو من الله أن يمد في عمرك لترى ثماراً قد حان قطافها بعد طول انتظار، وستبقى كلماتك نجوما أهتدي بها اليوم وفي الغد وإلى الأبد:

(والدي العزيز).

إلى من أرضعتني الحب والحنان، إلى رمز الحب وبلسم الشفاء، إلى القلب الناصع بالبياض، إلى من كان دعائها سر نجاحي، وحنانها بلسم جراحي:

(والدتي الحبيبة).

إلى القلوب الطاهرة الرقيقة، والنفوس البريئة، إلى رياحين حياتي:

(إخوتي).

وقبل أن نمضي، نقدم أسمى آيات الشكر، والامتنان، والتقدير، والمحبة، إلى الذين حملوا أقدس رسالة في الحياة، إلى الذين مهدوا لنا طريق العلم، والمعرفة، إلى جميع أساتذتنا الأفاضل، وأخص بالتقدير والشكر:

الدكتور/ الرضى محمد عباس

وكذلك نشكر كل من ساعد على إتمام هذا البحث، وقدم لنا العون، ومد لنا يد المساعدة، وزودنا بالمعلومات اللازمة؛ لإتمام هذا البحث ونخص بالذكر:

المهندس/ محمد ميرغنى.

م/ آدم حسان محمود الروم

TABLE OF CONTENTS

Contents	Page
DEDICATION	I
ABSTRACT	VIII
TABLE OF CONTENTS	III
LIST OF TABLE	V
LIST OF FIGURES	VI
 CHAPTER 1: INTRODUCTION	
1.1 General Introduction	1
1.2 Capillary Pressure in General	1
1.3 The Bentiu Formation	4
1.4 Effect of water cut	5
1.5 Water Saturations and Free Water Level	6
1.6 Problem Statement	7
1.7 Objectives	7
 CHAPTER 2: Theoretical Background and Literature Review	
2.1 Capillary Pressure Behavior	8
2.2 Surface and Interfacial Tension	11
2.3 Information about Bentiu	16
 CHAPTER 3: Methodology	
3.1 Core and log Petrophysics	18
3.1.1 Tack capillary pressure data from the laboratory.....	18

3.1.2 Convert laboratory capillary pressure data to reservoir capillary pressure data	18
3.1.3 Convert Leverett-J Function from P_c	19
3.1.4 Plot J-Function vs S_w denormalized and get new correlation	20
3.1.5 Convert J_{new} to $P_{c_{new}}$	20
3.1.6 Convert p_c to H	20
3.1.7 Determine the transition zone	20
CHAPTER 4: Calculation and Result	
4.1 The Capillary pressure data	21
4.2 Convert laboratory capillary pressure data to reservoir gas-brine capillary pressure data	22
4.3 Capillary pressure curves	23
4.4 Calculate Leverett-J function from P_c	24
4.5 Leverett J function model	26
4.6 From figure 4-3 we convert $P_{c_{new}}$ to High (H)	28
4.7 Log curve match	30
CHAPTER 5: Conclusion and Recommendation	
5.1 Conclusion	32
5.2 Recommendation	33
REFERENCES	34
Appendix	35

LIST OF TABLE

Tables	Page
Table 4-1 shows capillary pressure data from lab.....	21
Table4-2 interfacial tension and contact angel constants	22
Table 4-3 shows conversion of capillary pressure from lab data to reservoir data	23
Table 4-4 shows conversion of J – function	25
Table 4-5 shows J new and Pc new and H and Pd	28

LIST OF FIGURE

Figures	Page
Figure 1-1 Water saturation profile, (Tarek. A, 2010)	3
Figure 2-1 Pressure difference across a curved (spherical) interface	9
Figure 2-2 Pressure relation in capillary tubes, (Tarek. A, 2010)	11
Figure 2-3 Illustration of surface tension, (Tarek. A, 2010)	12
Figure 4-1 capillary pressure curve for core sample	24
figure 4-2 Relationship between J function and water Saturation	26
Figure 4-3 shows S_{wn} vs P_{cnew}	27
Figure 4-4 shows height (hm) vs saturation water (S_{wn})	29
Figure 4-5 represent log model from well X	30
Figure 4-6 represent log model from well Y	31
Figure A-1 shows the face of mat lab program	35
Figure A-2 shows the start of the entry	35
Figure A-3 shows enter value in program	36
Figure A-4 shows Enter values in program	37
Figure A-5 shows Enter values in program	38
Figure A-6 shows Results P_{cr} and Porosity avg. and permeability avg.	39
Figure A-7 shows Results J-function.	39
Figure A-8 shows relationship between S_w and P_{cr}	40
Figure A-9 shows relationship between S_w and J	40
Figure A-10 shows relationship between S_{wn} and P_{cn}	41
Figure A-11 shows transition zone and all previously result	41

Figure A-12 shows the codes of used	42
Figure A-13 shows the codes of used	43
Figure A-14 shows the codes of used	44

Abstract

The study of the physical properties of reservoir rocks and knowledge related accounts of great importance, As it relates to understanding the behavior of the fluid now inside the circles with respect to porosity' and size of the reserve accounts and assess the classes before the start of development processes.

This study addresses some of the physical properties of the rocks and in particular those that can be used in determining the oil water contact Determining the oil-water contact is very important in the assessment phase and class in determining the area of contact between the oil and the water and see the transition zone.

The study shows the estimation process of oil-water contact (OWC) and give best understanding of the capillary behavior of hydrocarbon reservoirs that are vital for optimum reservoir characterization. Hence, the height of oil-water contact above free water level for different rock types from some Sudanese field reservoirs were estimated.

The Data obtained from oil-displacing brine (drainage) capillary pressure tests using refined oil as simulated brine formation or reservoir fluid on various rock samples were utilized to illustrate the basic capillary behavior often hydrocarbon reservoirs and to estimate the (OWC) above Free Water Level.

The study shows that all the samples taken from bentiu formation show high permeability and well sorted grains which is indicative of good reservoirs this is further confirmed a depth range of 2998.5 to 3050 m which indicate good quality reservoirs.

Calculation result of the capillary model indicate that the oil water contact value at (3018m) (9899.04 ft) and from well logging at (3020.4m) (1050.912 ft)

التجريد

دراسة الخصائص الفيزيائية لصخور المكنم والحسابات المتعلقة بها ذات أهمية كبيرة، حيث أنها تتعلق بفهم سلوك المانع داخل المكنم فيما يتعلق بالمسامية وحجم المخزون النفطي وتقييم الطبقات قبل بداية عمليات التطوير.

تتناول هذه الدراسة بعض الخواص الفيزيائية للصخور، وخاصة تلك التي يمكن استخدامها في تحديد الخط الفاصل بين الماء والنفط، وتحديد هذا الفاصل مهم جدا في مرحلة التقييم والتصنيف، وفي تحديد المنطقة الانتقالية بين النفط والماء ويعتبر أمر حيوي لوصف الخزان الأمثل في عمليات الاستكشاف والإنتاج، وتقدير ارتفاع منسوب المياه فوق مستوى الماء الحر

تناولت الدراسة طرق حسابات الخط الفاصل باستخدام السلوك الشعري بالمقارنة مع نموذج تسجيلات الآبار للمكامن النفطية لمكنم نفطي سوداني.

تم استخدام بيانات من العينات الصخرية النفطية في اختبارات الضغط الشعري وتشبعات المياه المأخوذة من مختلف العينات؛ لتوضيح السلوك الشعري للطبقة الهيدروكربونية.

أُخذت العينات من طبقة بانتيو في الأعماق (2998,5 إلى 3050) متر و (3002,5 إلى 3050) متر أظهرت نفاذية ومسامية عالية، مما يدل على جودة الطبقة

وكان عمق الحد الفاصل بين النفط والماء المتحصل عليها من حسابات الضغط الشعري (3018 م) الذي يعادل (9899.04 قدم)، ومن نتائج تسجيلات الآبار (3020.4 م) الذي يعادل (1050.912 قدم).

Chapter one

Introduction

Chapter one

Introduction

1.1 General Introduction

The present worldwide daily water production from oil wells roughly high, although some wells produce significantly higher amounts. It costs money to lift water and then dispose of it. In a well producing oil with 80% water cut, the cost of handling water can double normal lifting costs. Yet, wells with water cuts in excess of 90% may still produce sufficient hydrocarbons to be economical. Water control technology is intended to reduce the costs of producing water.

It is not necessary, nor desirable, to completely shut off the coproduced water. The logic here is the distinction between “good” (necessary) and “bad” (excess) water. “Good” water is that water produced at a rate below the water/oil economic limit (i.e., the oil produced can pay for the water produced). “Good” water, then, is that water that cannot be shut off without reducing oil production. The fractional water flow is dictated by the natural mixing behavior that gradually increases water/oil ratio (WOR). “Good” water is also caused by converging flowlines from the injector to the producer wellbore. Water breakthrough on injection occurs initially along the shortest (least resistant) flow path between injector and producer, while oil is still being swept along other flow paths.

“Bad” water is water produced into the wellbore that produces no oil or insufficient oil to pay for the cost of handling the water. The remainder of this discussion deals with “bad” water.

1.2 Capillary Pressure In General

Capillary forces are one of effective parameters in hydrocarbon reservoirs which are notable in the porous media. Capillary pressure is one of input data in reservoir simulation process which should be considered in history matching procedures.

The capillary forces in a petroleum reservoir are the result of the combined effect of the surface and interfacial tensions of the rock and fluids, the pore size and geometry, and the wetting characteristics of the system. Any curved surface between two immiscible fluids has the tendency to contract into the smallest possible area per unit volume. This is true whether the fluids are oil and water, water and gas (even air), or oil and gas. When two immiscible fluids are in contact, a discontinuity in pressure exists between the two fluids, which depends upon the curvature of the interface separating the fluids. We call this pressure difference the *capillary pressure* and it is referred to by p_c .

The displacement of one fluid by another in the pores of a porous medium is either aided or opposed by the surface forces of capillary pressure. As a consequence, in order to maintain a porous medium partially saturated with non-wetting fluid and while the medium is also exposed to wetting fluid, it is necessary to maintain the pressure of the non-wetting fluid at a value greater than that in the wetting fluid.

Denoting the pressure in the wetting fluid by p_w and that in the non-wetting fluid by p_{nw} , the capillary pressure can be expressed as:

Capillary pressure = (pressure of the non-wetting phase) – (pressure of the wetting phase)

That is, the pressure excess in the nonwetting fluid is the capillary pressure, and this quantity is a function of saturation. This is the defining equation for capillary pressure in a porous medium, (Tarek. A, 2010).

There are three types of capillary pressure:

- Water-oil capillary pressure (denoted as P_{cwo})
- Gas-oil capillary pressure (denoted as P_{cgo})
- Gas-water capillary pressure (denoted as P_{cgw})

An important application of the concept of capillary pressures pertains to the fluid distribution in a reservoir prior to its exploitation. The capillary pressure-saturation data can be converted into height-saturation data.

Figure 1-1 shows a plot of the water saturation distribution as a function of distance from the free-water level in an oil-water system. It is essential at this point to introduce and define four important concepts:

- Transition zone
- Water-oil contact (WOC)
- Gas-oil contact (GOC)
- Free water level (FWL)

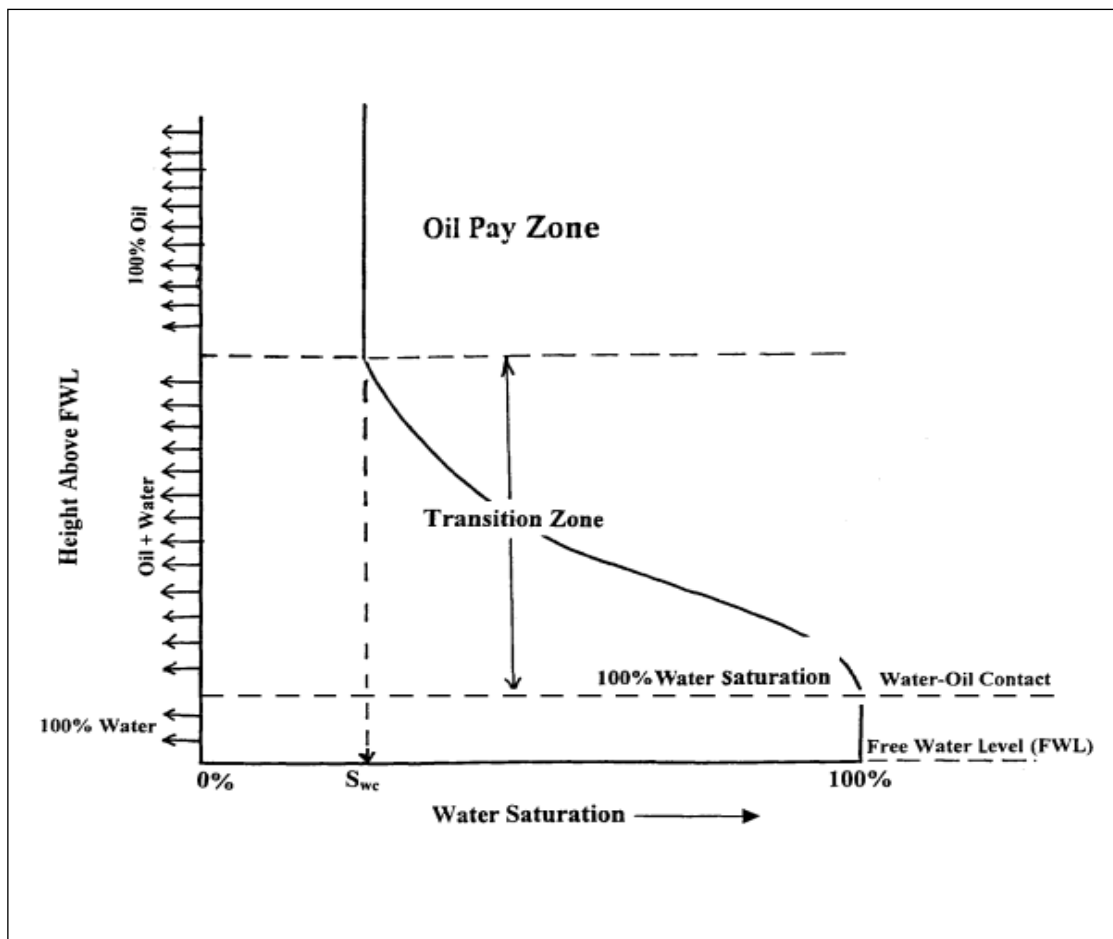


Figure 1-1: Water saturation profile, (Tarek. A, 2010).

In evaluating hydrocarbon reservoirs, laboratory capillary pressure measurements on reservoir cores are directly applied to determine basic petrophysical properties such as pore size distribution, irreducible water saturation, residual oil saturation, and wettability of reservoir rocks.

1.3 The Bentiu Formation

The Bentiu formation in the Muglad rift basin block-6, Sudan. The subsurface sediments were investigated essentially by two methods are wirelines log interpretation and core analysis.

The log interpretation of two wells (Fula-1, Fula-2) showed that the rock type is dominantly Sandstone and the dominant depositional regime is braided channel fluvial system. As well as, most of the Sandstone layers in Fula-1 containing hydrocarbons, and the Sandstone layers in Fula-2 is more contain hydrocarbons than Fula-2.

Megascopic core description and observation of sedimentary sequences were done before any other detailed analyses. The main types of facies are Conglomerates, Sandstones, Siltstones, Mudstones and Shales. From the lithofacies analysis of the conventional cores.

The minerals and components which are recognized in the thin sections include: Detrital components (quartz, feldspar, mica, lithics and detrital clays) and authigenic components (carbonates, quartz overgrowth, iron oxides cement and pyrite).

In this project, we focus on the detection and control of excess water production. First, we review the many ways in which water can enter the wellbore. Then, we describe measurements and analysis to identify these problem types. Finally, we examine treatments and solutions. Case studies demonstrate applications in individual wells, on a field scale and in surface facilities.

1.4 Effect of water cut

Water affects every stage of oilfield life from exploration—the oil-water contact is a crucial factor for determining oil-in-place—through development, production, and finally to abandonment.

As oil is produced from a reservoir, water from an underlying aquifer or from injectors eventually will be mixed and produced along with the oil. This movement of water flowing through a reservoir, into production tubing and surface processing facilities, and eventually extracted for disposal or injected for maintaining reservoir pressure, is called the ‘water cycle’.

Oil producers are looking for economic ways to improve production efficiency, and water-control services are proving to be one of the fastest and least costly routes to reduce operating costs and improve hydrocarbon production simultaneously.

The economics of water production throughout the water cycle depend on a number of factors such as total flow rate, production rates, fluid properties like oil gravity and water salinity, and finally the ultimate disposal method for the water produced. Operational expenses, including lifting, separation, filtering, pumping and reinjection, add to the overall costs.

In addition, water-disposal costs can vary enormously. Reports vary from 10 cents per barrel when the unwanted water is released into the ocean offshore to over \$1.50 per barrel when hauled away by trucks on land. Although the potential savings from water control alone are significant, the greatest value comes from the potential increase in oil production and recovery

1.5 Water Saturations and Free Water Level

Determining accurate water saturations (S_w) is important both for accurate volumetric calculations and for flow modeling, because water saturation can significantly influence gas relative permeability even in rocks at “irreducible” water saturation (S_{wi}).

It is well recognized for determination of formation water saturations from induction wireline log response is problematic. Traditional methods of determining water including routine core saturations and induction wireline log analysis are complicated by deep mud filtrate invasion resulting from the common drilling management practice of drilling with a large hydrostatic overbalance relative to low-pressure reservoirs.

Routine core water saturations are high due to flushing during the coring operation that is further enhanced by capillary imbibition of water due to low gas pressure in the core and high drilling mud pressure.

Because water saturations cannot be reliably determined for most wells using logs, it was decided to estimate water saturations based on matrix capillary-pressure properties and determination of the free water level (FWL, level at which gas-brine capillary pressure is zero).

Employed a capillary pressure, matrix-based methodology for predicting water saturations for intervals in the Chase.

1.6 Problem Statement

High water cut in Bentiu formation (X & Y Wells data) can be related to wrong determination of water oil contact, uncorrected perforation. Determination of formation water saturations from induction of wireline log response only can lead to bad diagnosis of determination water oil contact,. The research aim to verify the accurate water oil contact using both capillary model and log model

1.7 Objectives

1. Convert capillary pressure lab data to reservoir conditions.
2. Explain the relation between capillary pressure data and reservoir fluid saturation.
3. Sufficient Define of oil-water and gas-oil transition zones.
4. Sketch capillary pressure curves for typical drainage and imbibition processes.
5. Taken initial water saturation in the reservoir and Determine water oil contact.
6. verify the accurate water oil contact using both capillary model and log model

Chapter two

Theoretical background

And

Literature Review

2.1 Capillary Pressure Behavior

Capillary behavior is one of the most important factors which determine the distribution of hydrocarbon. Detailed understanding of the capillary force of a reservoir is therefore vital for effective reservoir characterization. The rise of water in the capillary tube experiment is initiated by a capillary force. This force is balanced by the weight of the rising liquid. The same principle governs the migration of hydrocarbons in porous reservoirs which may be viewed as a bundle of straight cylindrical capillaries with varying diameters. In this model, the oil, water contact (O WC) is the depth at which oil and water start entering the pores in the rock.

Thus, it is the depth below which water saturation is 100%. The zone of 100% water saturation exists above the free water level (FWL). The (OWC) in a reservoir is dependent on lithology or formation strata of the field.

Estimate and recognition of fluid contacts such as oil water contact (OWC) in reservoirs are essentials for reservoir characterization and evaluation of hydrocarbon in place (Acher, 1986) and (Adam, 1993).

When two immiscible fluids are in contact in the interstices of a porous medium, a discontinuity in pressure exists across the interface separating them. The difference in pressure P_c is called capillary pressure (Figure 2-1) which is pressure in the non-wetting phase minus the pressure in the wetting phase.

Capillary pressure = (pressure of the non-wetting phase) – (pressure of the wetting phase)

$$P_c = P_{nw} - P_w \quad (2.1)$$

That is, the pressure excess in the non-wetting fluid is the capillary pressure, and this quantity is a function of saturation. This is the defining equation for capillary pressure in a porous medium, (O. Torsaeter, 2003).

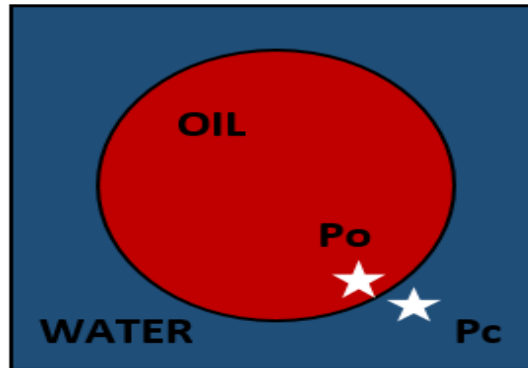


Figure 2-1: Pressure difference across a curved (spherical) interface.

Applying the mathematical definition of the capillary pressure as expressed by Equation (2-1), the three types of the capillary pressure can be written as:

$$P_{cwo} = P_o - P_w \quad (2-2)$$

$$P_{cgo} = P_g - P_o \quad (2-3)$$

$$P_{cgw} = P_g - P_w \quad (2-4)$$

Where P_g , P_o , and P_w represent the pressure of gas, oil, and water, respectively.

If all the three phases are continuous, then:

$$P_{cgw} = P_{cgo} + P_{cwo} \quad (2-5)$$

Referring to Figure 2-2, the pressure difference across the interface between Points 1 and 2 is essentially the capillary pressure, i.e.:

$$P_c = P_1 - P_2 \quad (2-6)$$

The pressure of the water phase at Point 2 is equal to the pressure at point 4 minus the head of the water, or:

$$P_2 = P_4 - g h_{pw} \quad (2-7)$$

The pressure just above the interface at Point 1 represents the pressure of the air and is given by:

$$P_1 = P_3 - gh\rho_{\text{air}} \quad (2-8)$$

It should be noted that the pressure at Point 4 within the capillary tube is the same as that at Point 3 outside the tube. Subtracting Equation (2-7) from (2-8) gives:

$$P_c = gh(\rho_w - \rho_{\text{air}}) = gh\Delta\rho \quad (2-9)$$

Where $\Delta\rho$ is the density difference between the wetting and non-wetting phase. The density of the air (gas) is negligible in comparison with the water density. In practical units, Equation (2-9) can be expressed as:

$$P_c = \left(\frac{h}{144}\right)\Delta\rho \quad (2-10)$$

Where :

P_c = capillary pressure, psi

h = capillary rise, ft

$\Delta\rho$ = density difference, lb/ft³

In the case of an oil-water system, Equation (2-9) can be written as:

$$P_c = gh(\rho_w - \rho_o) = gh\Delta\rho \quad (2-11)$$

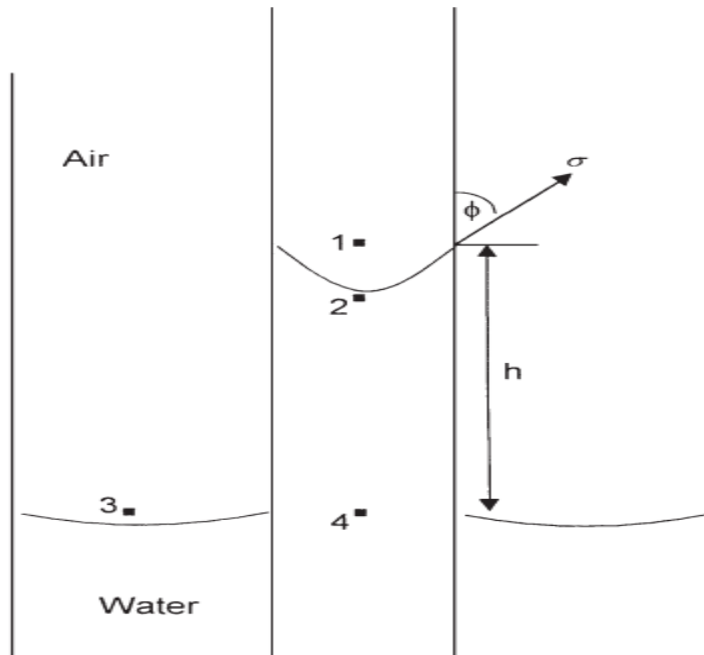


Figure 2-2: Pressure relation in capillary tubes, (Tarek. A, 2010)

2.2 Surface and Interfacial Tension

In dealing with multiphase systems, it is necessary to consider the effect of the forces at the interface when two immiscible fluids are in contact. When these two fluids are liquid and gas, the term *surface tension* is used to describe the forces acting on the Interfacial tension.

Surfaces of liquids are usually blanketed with what acts as a thin film. Although this apparent film possesses little strength, it nevertheless acts like a thin membrane and resists being broken. This is believed to be caused by attraction between molecules within a given system. All molecules are attracted one to the other in proportion to the product of their masses and inversely as the squares of the distance between them.

Consider the two immiscible fluids, air (or gas) and water (or oil) as shown schematically in Figure 2-3. A liquid molecule, which is remote from the interface, is surrounded by other liquid molecules, thus having a resulting net attractive force on the molecule of zero. A molecule at the interface, however, has a force acting on it from the air (gas) molecules lying immediately above the interface and from liquid molecules lying below the interface (Tarek. A, 2010).

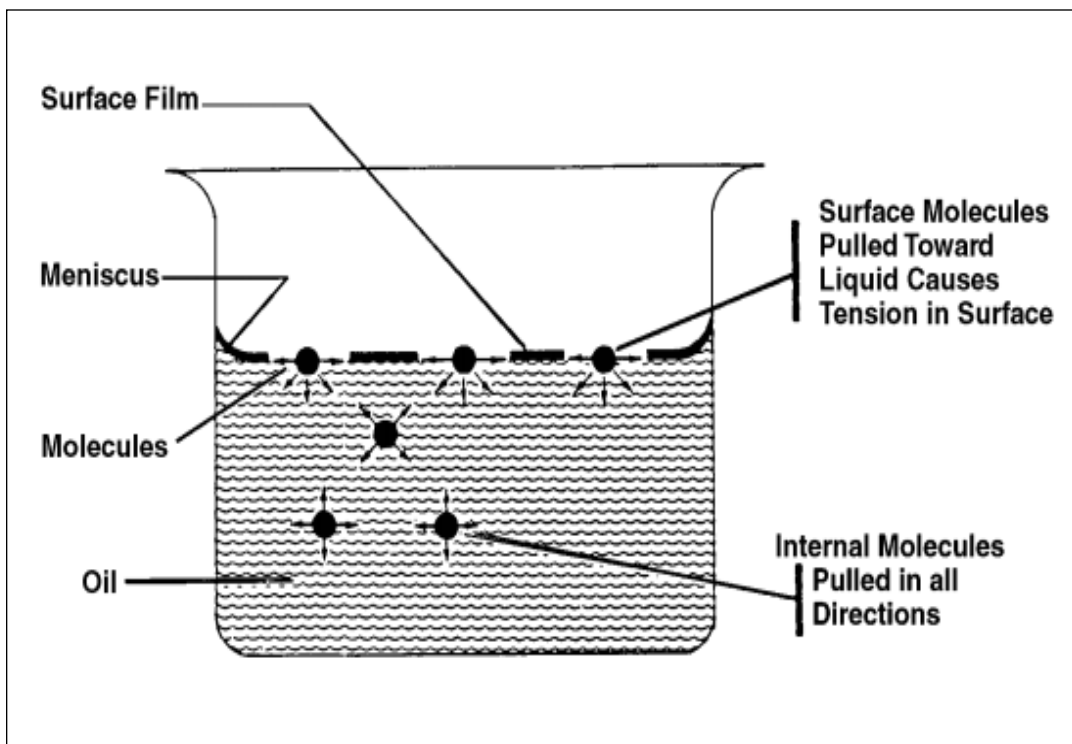


Figure 2-3: Illustration of surface tension,
(Tarek. A, 2010).

The surface or interfacial tension has the units of force per unit of length, e.g., dynes/cm, and is usually denoted by the symbol σ .

If a glass capillary tube is placed in a large open vessel containing water, the combination of surface tension and wettability of tube to water will cause water to rise in the tube above the water level in the container outside the tube as shown in Figure 2-2.

The water will rise in the tube until the total force acting to pull the liquid upward is balanced by the weight of the column of liquid being supported in the tube. Assuming the radius of the capillary tube is r , the total upward force F_{up} , which holds the liquid up, is equal to the force per unit length of surface times the total length of surface, or

$$F_{up} = (2\pi r) (\sigma_{gw}) (\cos \theta) \quad (2-12)$$

Where:

σ_{gw} : surface tension between air (gas) and water (oil), dynes/cm

θ : contact angle

r : radius, cm

The upward force is counteracted by the weight of the water, which is equivalent to a downward force of mass times acceleration,

Or

$$F_{down} = \pi r^2 h (\rho_w - \rho_{air}) g \quad (2-13)$$

Where:

h : height to which the liquid is held, cm

g : acceleration due to gravity, cm/sec²

ρ_w : density of water, gm/cm³

ρ_{air} : density of gas, gm/cm³

Because the density of air is negligible in comparison with the density of water, Equation (2-13) is reduced to:

$$F_{down} = \pi r^2 \rho_w g \quad (2-14)$$

Equating Equation (2-12) with (2-14) and solving for the surface tension gives:

$$\sigma_{gw} = \frac{r h \rho_w g}{2 \cos \theta} \quad (2-15)$$

The generality of Equations (2-12) through (2-15) will not be lost by applying them to the behavior of two liquids, i.e., water and oil. Because the density of oil is not negligible, Equation (2-15) becomes:

$$\sigma_{wo} = \frac{rhg(\rho_w - \rho_o)}{2\cos\theta} \quad (2-16)$$

Where:

ρ_o : density of oil, gm/cm³

σ_{ow} : interfacial tension between the oil and the water, dynes/cm

The capillary pressure equation can be expressed in terms of the surface and interfacial tension by combining Equations (2-9) and (2-11) with Equations (2-15) and (2-16) to give:

• **Gas-liquid system**

$$P_c = \frac{2\sigma_{gw}(\cos\theta)}{r} \quad (2-17)$$

and

$$h = \frac{2\sigma_{gw}(\cos\theta)}{rg(\rho_w - \rho_{gas})} \quad (2-18)$$

Where :

ρ_w : water density, gm/cm³

σ_{gw} : gas-water surface tension, dynes/cm

r : capillary radius, cm

θ : contact angle

h : capillary rise, cm

g : acceleration due to gravity, cm/sec²

P_c : capillary pressure, dynes/cm²

• **Oil-water system**

$$P_c = \frac{2\sigma_{ow}(\cos\theta)}{r} \quad (2-19)$$

and

$$h = \frac{2\sigma_{wo}(\cos\theta)}{rg(\rho_w - \rho_{gas})} \quad (2-20)$$

Where:

σ_{wo} is the water-oil interfacial tension. (Tarek. A, 2010).

The conversion of laboratory-measured capillary pressure to equivalent reservoir gas column height above free water level requires the input of a range of fluid properties including interfacial tension, contact angle, and density. Because these properties change with gas and brine composition and reservoir pressure and temperature.

The proper knowledge of the petrophysical properties of a reservoir depends on the investment in coring or well logging. Logging allows the access to physical data of the formations while drilling occurs, sending it to the surface to be analyzed through the drilling fluid. All the data helps formation evaluation.

The purpose of well logging is the acquisition of physical data of the formations drilled in order to figure out where the pay zones are. A pay zone is a hydrocarbon rich formation which can be explored with profit. A formation with pay zone characteristics is porous, permeable and saturated with hydrocarbons, so logging's final objective is the estimation of the porosity, permeability and saturation of the formations.

Logging tools acquire data concerning the resistivity, gamma ray emission, neutron interaction, density, seismic wave velocity, temperature, inclination and azimuth of the formations.

These tools are nowadays mostly placed in the bottom-hole assembly, 3 to 20 meters above the drill bit and measure the properties of the formations as the bit advances, in a practice known as Logging While Drilling (Hearst et al., 2000).

Not only the inclination and azimuth of the formations is measured, the orientation of the bit is measured and corrected with the help of a technique called **Measurement While Drilling**. MWD helps the driller reaching his objective in horizontal wells. Both LWD and *MWD data is transferred to the surface through the drilling fluid column in wave form, although most of it is saved for posterior analysis.*

For log interpretation, invasion modeling by George et al. (2004) examined the complexity of the mud-filtrate invasion process and the influence of a low-resistivity mud-filtrate annulus on induction log response.

Their study indicated that modeling of invasion is required to estimate gas saturation and that there is no simple procedure to correct previously acquired logs. Using conventional saturation calculation methods, calculated water saturations are significantly higher than true formation saturations.

2.3 Information about Bentiu

Hanan (1997) investigated in her study Cenomanian-Late Albian continental fluvial Bentiu formation based on data obtained from three exploration wells, in W Muglad basin. Various methods have been used in the present work including lithofacies, reservoir quality, heavy mineral and clay mineral analyses. The lithofacies analysis allowed the subdivision of Bentiu Formation into lower, middle and upper parts.

The stratigraphic change of lithological facies and depositional patterns of Bentiu formation reflect mainly both alicyclic and auto cyclic controls such as the tectonic activity, climate, drainage system, dispersal pattern and sediment load. Reservoir quality of Bentiu formation is controlled by grain-size and sorting and hence by depositional facies and environments. The facies analysis of Bentiu formation suggests a change in fluvial architecture and sand body geometry, from isolated, vertically stacked, narrow channels, in lower Bentiu

formation, to vertically stacked broad channels and sand sheets, in middle and upper Bentiu Formation.

It has been found that higher porosity and permeability values are associated with the coarse-grained sandy bedload dominated facies of upper and middle Bentiu Formation. In contrast, relatively lower porosity and permeability values are associated with the high sinuosity, mixedload meandering stream of lower Bentiu Formation. The heavy mineral analysis which was carried out on the whole penetration thickness of Abu Sufyan well reveals four distinct zones. The metamorphic rocks are the main contribtional source rock, in addition to the volcanic, plutonic igneous rocks and older sedimentary rocks. The heavy mineral assemblages were affected mainly by tectonism, weathering, transportation, abrasion and intrastratal solution. The clay minerals of Bentiu formation mainly consist of kaolinite, smectite, illite, mixed layer s/i and minor chlorite. The clay mineral assemblages of lower, middle and upper Bentiu Formation show a relationship with lithofacies types and depositional systems.

Chapter Three

Methodology

3.1 Core and log Petrophysics

Illustrated the limitations of determining water saturation from induction wireline logs and the inability to accurately use existing logs. Based on these results, analysis of electrical wireline log response to determine water saturation was not investigated further.

The physics governing determining water saturation from capillary pressure is well documented by these steps:

3.1.8 Take capillary pressure data from the laboratory.

The capillary forces in a petroleum reservoir are the result of the combined effect of the surface and interfacial tensions of the rock and fluids, the pore size and geometry, and the wetting characteristics of the system. Any curved surface between two immiscible fluids has the tendency to contract into the smallest possible area per unit volume.

This is true whether the fluids are oil and water, water and gas (even air), or oil and gas. When two immiscible fluids are in contact, a discontinuity in pressure exists between the two fluids, which depends upon the curvature of the interface separating the fluids. We call this pressure difference the capillary pressure and it is referred to by p_c .

3.1.9 Convert laboratory capillary pressure data to reservoir capillary pressure data

using the standard equation:

$$P_{c_{res}} = (\sigma_{res} \cos \theta_{res} / \sigma_{lab} \cos \theta_{lab}) P_{c_{lab}} \quad (3.1)$$

Where :

$P_{c_{res}}$: is the capillary pressure (psia) at reservoir conditions.

$P_{c_{lab}}$: is the laboratory-measured capillary pressure (psia).

$\sigma_{\text{res}}\cos\theta_{\text{res}}$: is the interfacial tension (σ , dyne/cm) times the cosine of the contact angle (θ , degrees) at reservoir conditions.

$\sigma_{\text{lab}}\cos\theta_{\text{lab}}$: is the interfacial tension times the cosine of the contact angle at laboratory conditions.

3.1.10 Convert Leverett-J Function from Pc

Capillary pressure data are obtained on small core samples that represent an extremely small part of the reservoir and, therefore, it is necessary to combine all capillary data to classify a particular reservoir. The fact that the capillary pressure-saturation curves of nearly all naturally porous materials have many features in common has led to attempts to devise some general equation describing all such curves.

Leverett (1941) approached the problem from the standpoint of dimensional analysis. Realizing that capillary pressure should depend on the porosity, interfacial tension, and mean pore radius, Leverett defined the dimensionless function of saturation, which he called the J-function,

an equation:

$$J = 0.21645 (Pc / \sigma \cos\theta) (K / \phi)^{0.5} \quad (3.2)$$

Where :

J : Leverett J-function

pc : capillary pressure, psi

σ : interfacial tension, dynes/cm

k : permeability, md

ϕ : fractional porosity

In doing so, Leverett interpreted the ratio of permeability, k, to porosity, ϕ , as being proportional to the square of a mean pore radius. The J-function was originally proposed as a means of converting all capillary-pressure data to a universal curve. There are significant differences in correlation of the J-function with water saturation from formation to formation, so that no universal curve can be obtained.

For the same formation, however, this dimensionless capillary-pressure function serves quite well in many cases to remove discrepancies in the p_c versus S_w curves and reduce them to a common curve.

3.1.4 Plot J-Function vs S_w denormalized and get new correlation.

$$J_{\text{new}} = 0.0581 (S_w)^{-3.623} \quad (3.3)$$

3.1.5 Convert J_{new} to P_c from equation:

$$J = 0.21645 (P_c / \sigma \cos \theta) (K / \phi)^{0.5} \quad (3.4)$$

Solving for P_c

$$P_c = J * (\sigma \cos \theta) * (K / \phi)^{0.5} / 0.21645 \quad (3.5)$$

3.1.6 Convert p_c to H from Equation:

$$H = 144 P_c / (\rho_w - \rho_o) \quad (3.6)$$

Where:

H: height above the free-water level, ft.

P_c : capillary pressure, psia.

$(\rho_w - \rho_o)$: density difference between the wetting and nonwetting phase, lb/ft³.

3.1.7 Determine the transition zone

From equation:

$$\text{Transition zone} = 144 (P_c - P_d) / (\rho_w - \rho_o) \quad (3.7)$$

Where:

P_d : displacement pressure, ps

Chapter Four

Calculation

And

Result

4.1 The Capillary pressure data

Capillary pressure data of 4 core samples Reservoirs obtained from Bentiu Formation in (X &Y wells) in south west of Sudan were used in this study.

A correlation was made between capillary model and log model to get OWC accurately.

Sample Number	k mD	phi frac	Pc lab PSI	Sw %
66 DEPTH : 3002.22 (m)	4.7	0.123	1	93.0
			4	79.5
			10	63.0
			30	55.8
			60	51.9
			100	49.0
			200	44.5
78 DEPTH : 3008.6 (m)	835	0.184	1	90.0
			4	58.4
			10	35.6
			30	27.1
			60	24.2
			100	22.2
			200	19.0
85 DEPTH : 3010.1 (m)	2078	0.235	1	87.2
			4	47.3
			10	26.3
			30	19.8
			60	18.0
			100	16.1
			200	14.0
95 DEPTH : 3013.35 (m)	1.83	0.113	1	95.8
			4	82.0
			10	69.2
			30	61.0
			60	56.0
			100	52.4
			200	47.4

Table 4-1: shows capillary pressure data from lab.

4.2 Convert laboratory capillary pressure data to reservoir gas-brine capillary pressure data

Using the standard equation (Purcell and Berg).

From

$$P_{\text{Cres}} = (\sigma_{\text{res}} \cos \theta_{\text{res}} / \sigma_{\text{lab}} \cos \theta_{\text{lab}}) P_{\text{Clab}} \quad (4-1)$$

System	Contact angle (θ)	Cosine contact(θ)	Interfacial tension T	T cosine θ
Laboratory				
Air water	0	1	72	72
Oil water	30	0.866	48	42
Air mercury	140	0.765	480	367
Air oil	0	1	24	24
Reservoir				
Water oil	30	0.866	30	26
Water gas	0	1	50	50

Table4-2: interfacial tension and contact angel constants

From this table we take air water from Laboratory and water oil from reservoir.

These are the result:

N	Sw fraction	Pc res psi	N	Sw fraction	Pc res psi
1	0.93	0.361	8	0.9	0.361
2	0.795	1.443	9	0.584	1.443
3	0.63	3.608	10	0.356	3.608
4	0.558	10.825	11	0.271	10.825
5	0.519	21.651	12	0.242	21.651
6	0.49	36.084	13	0.222	36.084
7	0.445	72.169	14	0.19	72.169
N	Sw fraction	Pc res psi	N	Sw fraction	Pc res psi
15	0.872	0.361	22	0.958	0.361
16	0.473	1.443	23	0.82	1.443
17	0.263	3.608	24	0.692	3.608
18	0.198	10.825	25	0.61	10.825
19	0.18	21.651	26	0.56	21.651
20	0.161	36.084	27	0.524	36.084
21	0.14	72.169	28	0.474	72.169

Table 4-3 shows conversion of capillary pressure from lab data to reservoir data.

4.3 Capillary pressure curves

All of capillary pressure raw data were converted to oil – water reservoir system by using equation (4-1)

The interfacial tension and contact angel which were used in this study are:

Interfacial tension (σ) = 72 dyne/ cm

Contact angel (θ) =30

Figure 4-1 show the drainage capillary pressure versus water saturation of core sample.

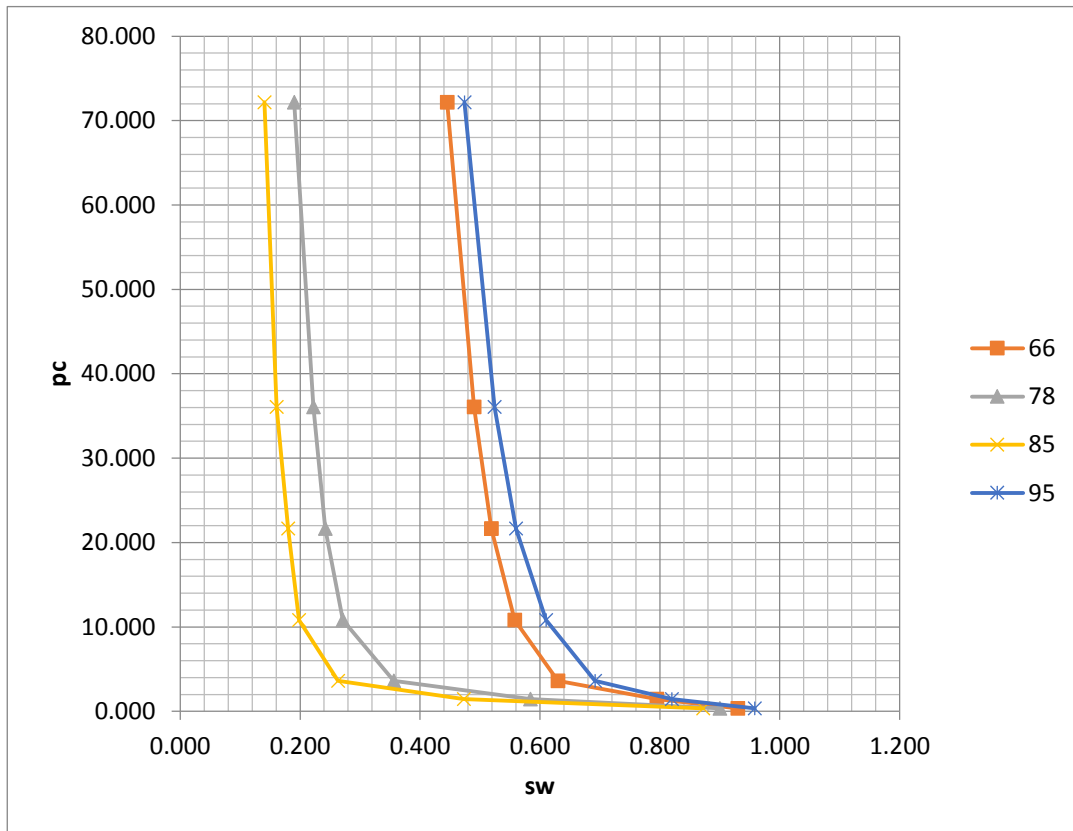


Figure 4-1 capillary pressure curve for core sample

4.4 Calculate Leveret-J function from Pc:

From this equation:

$$J = 0.21645 (P_c / \sigma \cos \theta) (K_{avr} / \phi_{avr})^{0.5} \quad (4-2)$$

$$K_{avr} = (k_1 * k_2 * \dots * k_n)^{1/n} \quad (4-3)$$

$$\Phi_{avr} = (\Phi_1 + \Phi_2 + \Phi_3 + \dots + \Phi_n) / n \quad (4-4)$$

N	sw	J-Function	N	sw	J-Function
1	0.93	0.018603	15	0.872	0.282692
2	0.795	0.074412	16	0.473	1.130769
3	0.63	0.18603	17	0.263	2.826923
4	0.558	0.55809	18	0.198	8.480768
5	0.519	1.11618	19	0.18	16.96154
6	0.49	1.8603	20	0.160517	28.26923
7	0.445	3.7206	21	0.140221	56.53845
8	0.9	0.202516	22	0.958	0.012098
9	0.584	0.810064	23	0.82	0.048392
10	0.356	2.02516	24	0.692	0.120979
11	0.271	6.075481	25	0.61	0.362938
12	0.242	12.15096	26	0.56	0.725876
13	0.222	20.2516	27	0.524	1.209794
14	0.190161	40.50321	28	0.474	2.419588

Table 4-4 shows conversion of J – function

4.5 Leveret J function model

In figure 4-2 the capillary pressure raw data of 4 samples converted to J-function values verses water saturation (SW) are plotted on seme-log plot relationship was found between water saturation and J-function.

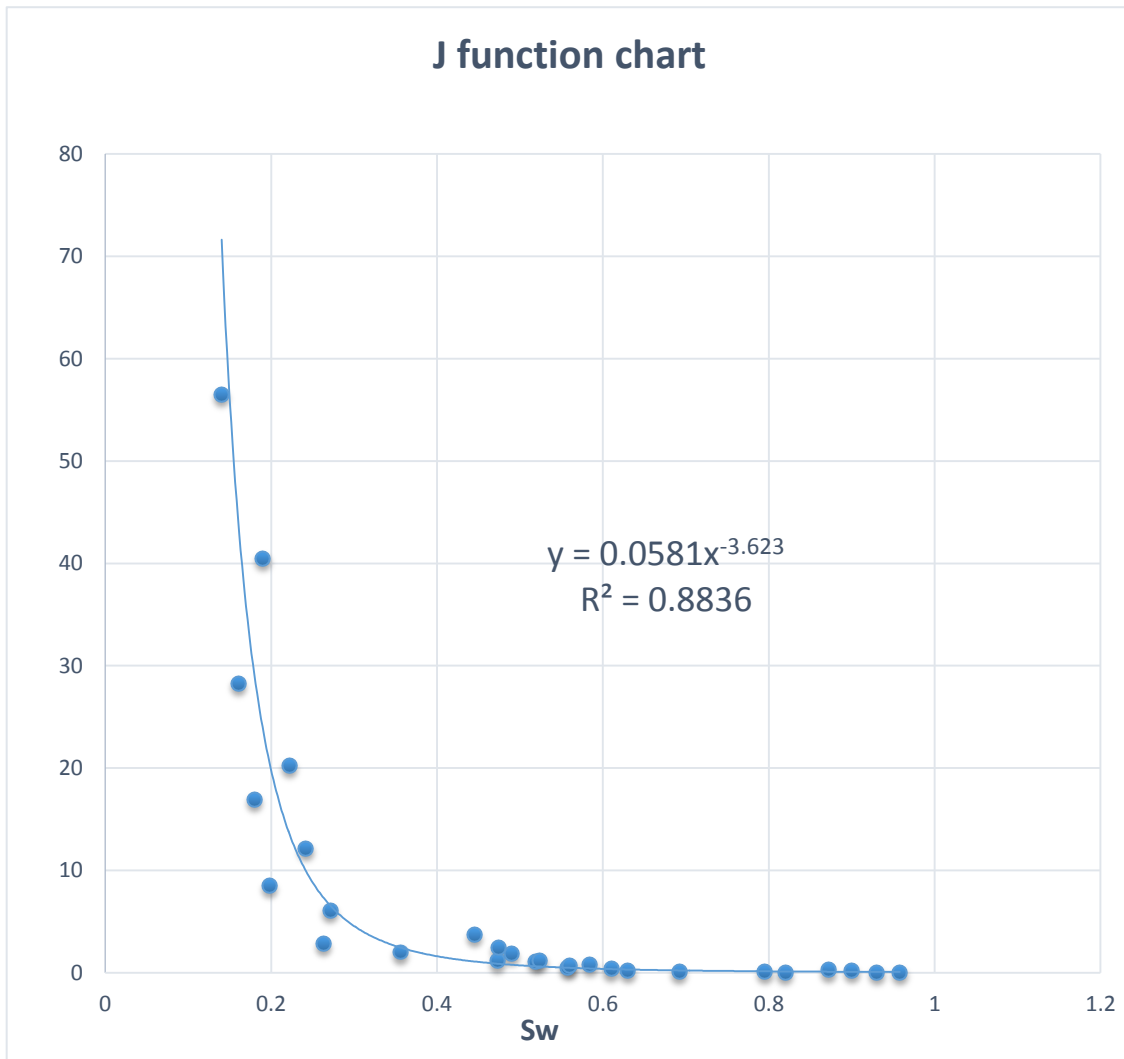


figure 4-2 Relationship between J function and water Saturation

From figure 4-2 we got J new from chart The equation is:

$$y = 0.0581x^{-3.623} \quad (4-5)$$

Where:

Y: J function

X: saturation water (sw)

$\rho_o=43.7$ lb/cu.ft

$\rho_w=64.1$ lb/cu.ft

We obtained pcnew from equation

$$P_c = J_{new} (\sigma \cos \theta) (K_{avg} / \phi_{avg})^{0.5} / 0.21645 \quad (4-6)$$

From this chart we obtained pd and pc

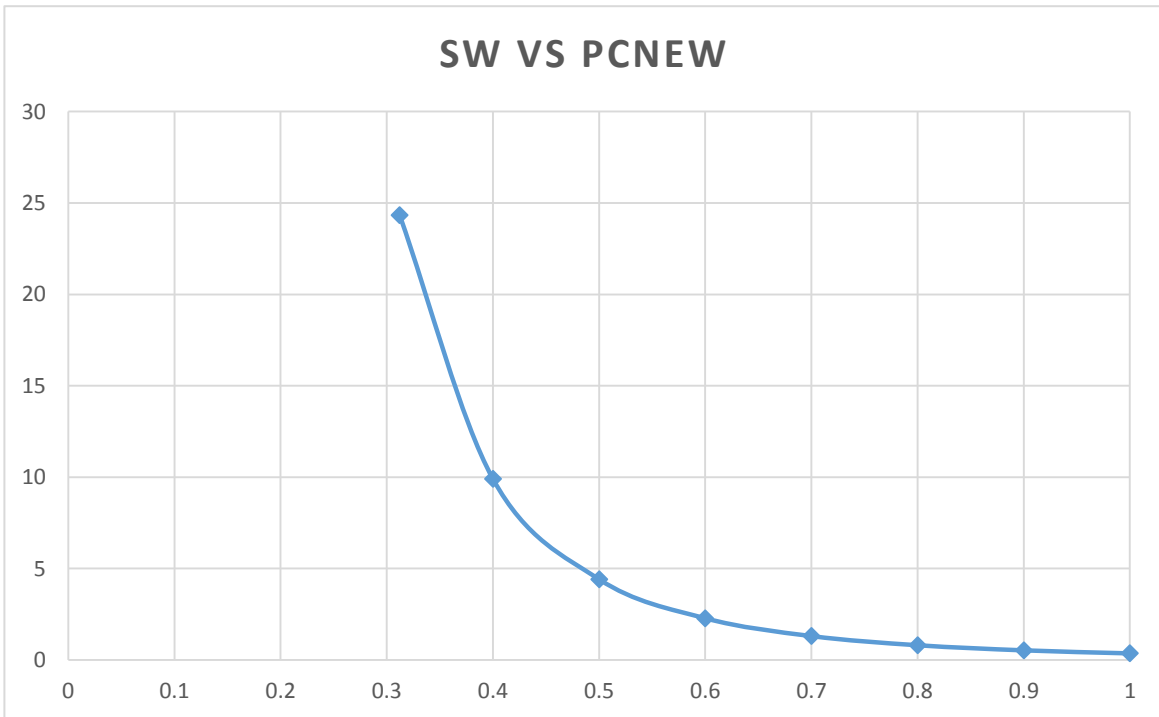


Figure 4-3 shows Swn vs pcne

Result:

$P_c = 10$ psi

$P_d = 0.358122859$ psi

4.6 From figure 4-3 we convert P_{cnew} to High (H)

From equation:

$$H = 144 * P_c / (\rho_w - \rho_o) \quad (4-7)$$

H: height above free water level

P_c : new capillary pressure, psi

P_d : displacement pressure, psi

Sw	J new	Pc new	h ft	h m	pd
1	0.0581	0.358122859	3.353036	1.022267	0.358123
0.9	0.085105	0.524579641	4.911539	1.49742	0.358123
0.8	0.130401	0.803779675	7.525635	2.294401	0.358123
0.7	0.211537	1.303892671	12.2081	3.721981	0.358123
0.6	0.369772	2.279240026	21.34009	6.506125	0.358123
0.5	0.715827	4.412286631	41.3114	12.59494	0.358123
0.4	1.606619	9.903043676	92.7203	28.26839	0.358123
0.31207645	3.948831	24.34021814	227.8928	69.47952	0.358123

Table 4-5 shows J new and P_{cnew} and H and P_d

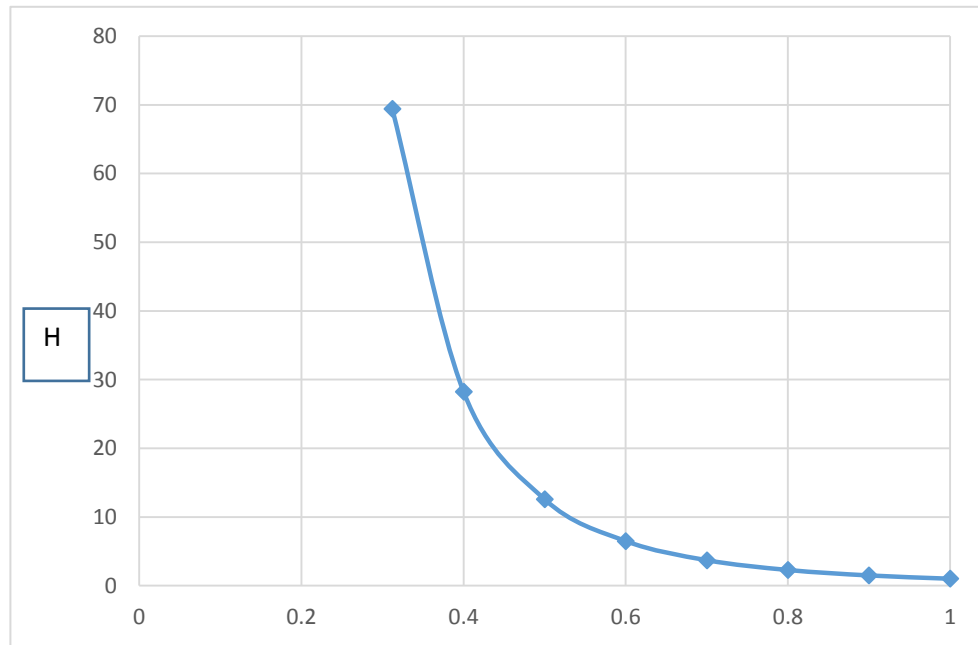


Figure 4-4 shows height (hm) vs saturation water (S_{wn})

From 4-4 we can obtain on transition zone depended on from eqation (4-7)

$$\text{Transition zone} = 144 * (\text{pc chart} - \text{pd chart}) / (\rho_w - \rho_o) \quad (4-8)$$

$$= 144 * (10 - 0.358122859) / (64.1 - 43.7)$$

$$\text{Transition zone} = 68.0603 \text{ ft} = 20.7\text{m}$$

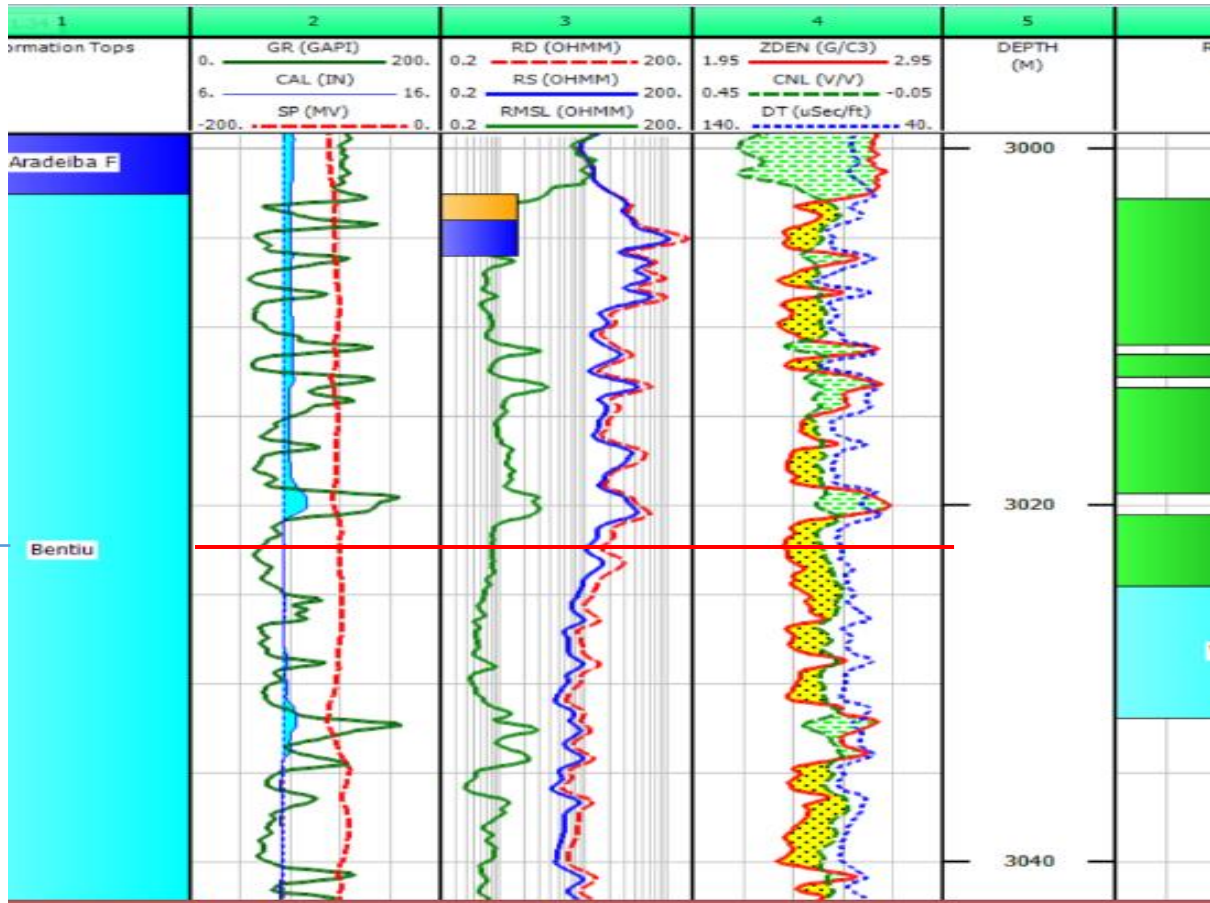
4.7 Log curve mach

Bentiu

3002.5-3050 m

WOC = 3024.6 m

Figure 4-5 represent log model from well X



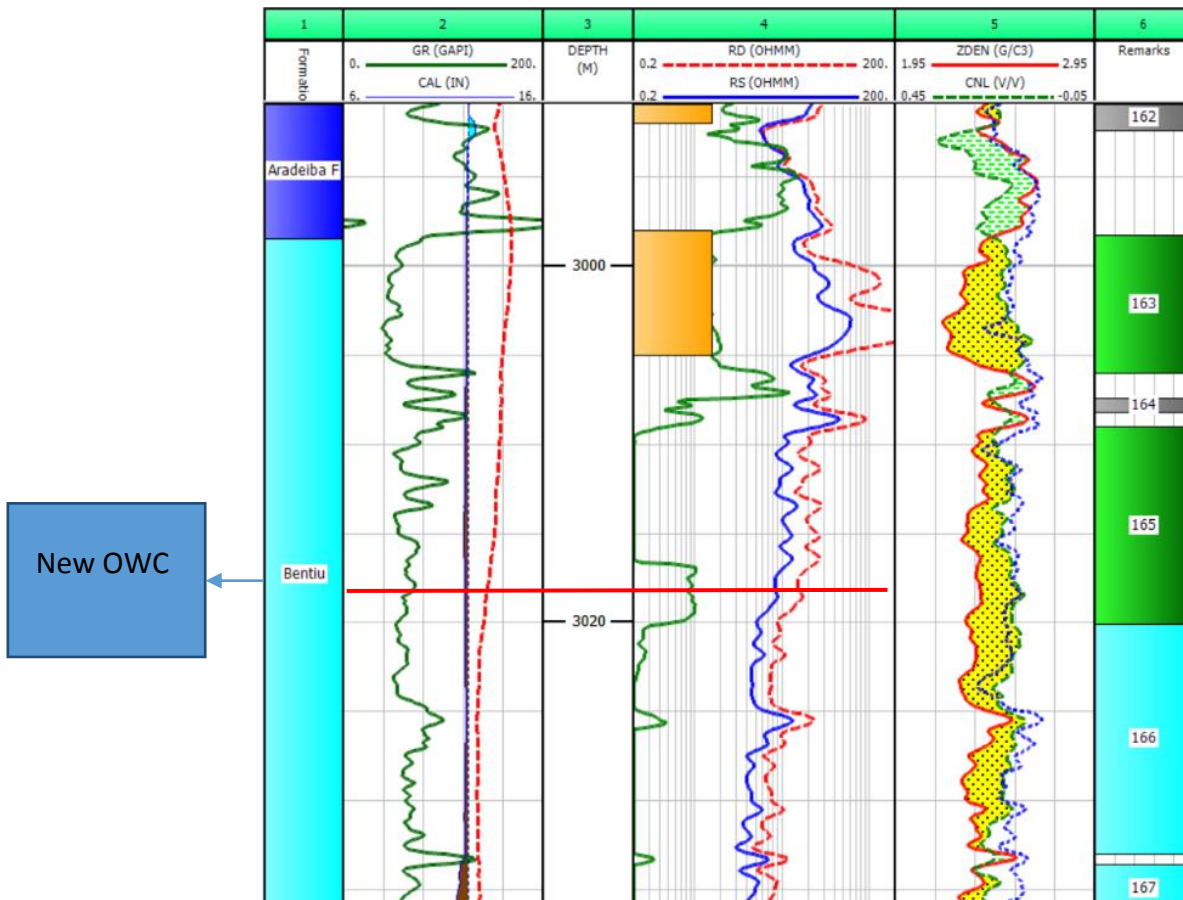
Mach between transition zone obtained on log model and capillary model

Bentiu

2998.5-3050 m

WOC = 3020.4 m

Figure 4-6 represent log model from well Y



Mach between transition zone obtained on log model and capillary model

Chapter five

Conclusion

And

Recommendation

5.1 Conclusion

Calculation value of the oil water contact were (3018m) (9899.04 ft) and data well Y logging (3020m) (1050.912 ft)

Calculation value of the oil water contact were (3022m) (9912.16 ft) and data well X logging (3024m) (9918.72ft)

The variation between log model and capillary model is (2m) (6.56 ft)

5.2 Recommendation

From the previous results we found that there is a difference in determination of water oil contact between pressure data and log data.

So it needs more study to reduce high water cut.

Use Repeat Formation Tester (RFT) for better results

References

- Adams, S _ J (1993): Capillary Pressure and Saturation Height Functions. Shell International Petroleum Maatschappij B.V. The Hague 5-6, 51-53, 76-79.
- Archer J. S (1986): Petroleum Engineering Principles and Practice. London: Gray and Trotman, Pages 10, 92-100.
- Bailey, B. 2000. Water Control. Oilfield Review 12 (1): 30.
- Central petroleum laboratory (CPL).
- Tarek Ahmed, (2010), Reservoir Engineering Handbook -4th Edition, Gulf Professional Publishing, 30 Corporate Drive, Suite 400, Burlington, MA 01803, USA.
- O. Torsæter, M. Abtahi, (2003), Experimental Reservoir Engineering laboratory Work Book, Norwegian University of Science and Technology.

Appendix

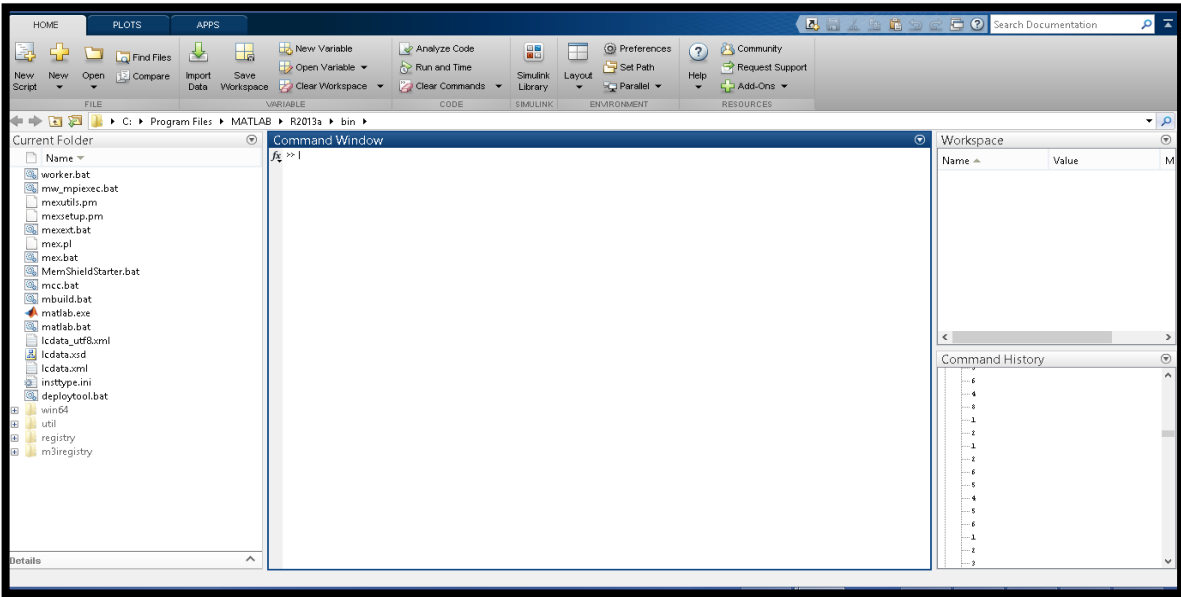


Figure A-1 shows the face of mat lab program

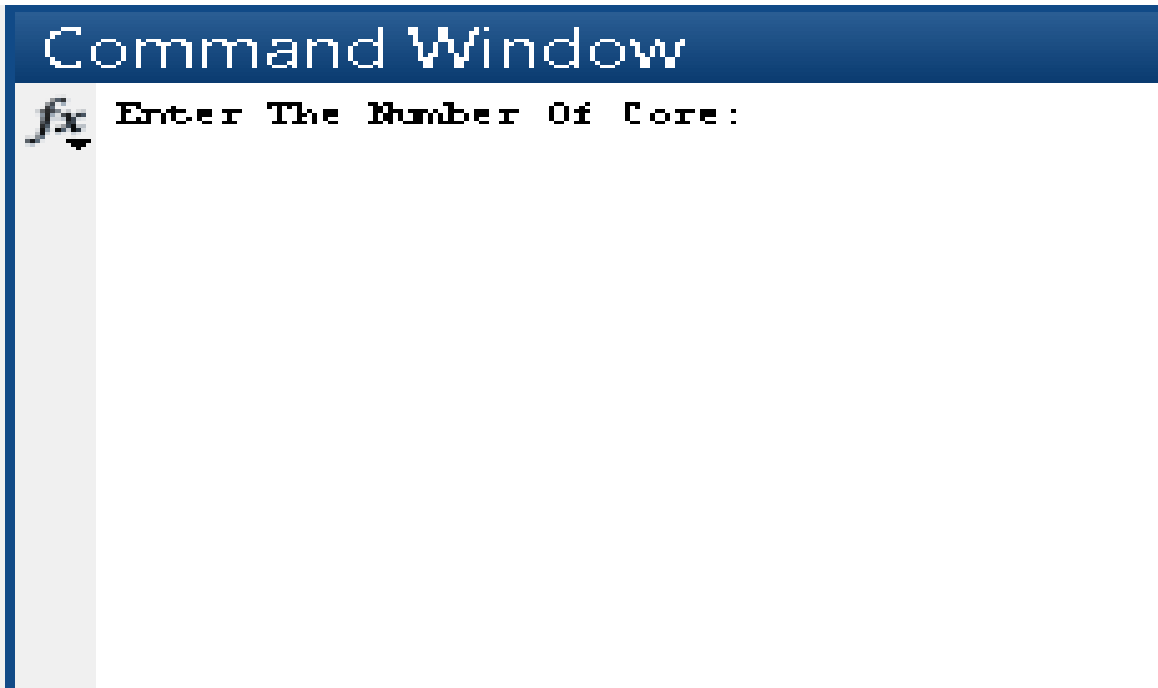


Figure A-2 shows the start of the entry

Command Window

```
Enter The Number Of Core:      4
Enter The Number Of row:      7
core(1)  row(1)
Enter Pc Lab Value:      1
Enter S0 Fraction Value:    .930
core(1)  row(2)
Enter Pc Lab Value:      4
Enter S0 Fraction Value:    .795
core(1)  row(3)
Enter Pc Lab Value:     10
Enter S0 Fraction Value:    .630
core(1)  row(4)
Enter Pc Lab Value:     20
Enter S0 Fraction Value:    .558
core(1)  row(5)
Enter Pc Lab Value:     60
Enter S0 Fraction Value:    .519
core(1)  row(6)
Enter Pc Lab Value:    100
Enter S0 Fraction Value:    .490
core(1)  row(7)
Enter Pc Lab Value:    200
Enter S0 Fraction Value:    .445
core(2)  row(1)
Enter Pc Lab Value:      1
Enter S0 Fraction Value:    .900
core(2)  row(2)
Enter Pc Lab Value:      4
Enter S0 Fraction Value:    .584
core(2)  row(3)
Enter Pc Lab Value:     10
Enter S0 Fraction Value:    .356
core(2)  row(4)
Enter Pc Lab Value:     30
Enter S0 Fraction Value:    .271
core(2)  row(5)
Enter Pc Lab Value:     60
Enter S0 Fraction Value:    .242
core(2)  row(6)
Enter Pc Lab Value:    100
Enter S0 Fraction Value:    .222
core(2)  row(7)
Enter Pc Lab Value:    200
Enter S0 Fraction Value:    .190
core(3)  row(1)
Enter Pc Lab Value:      1
Enter S0 Fraction Value:    .872
core(3)  row(2)
Enter Pc Lab Value:      4
Enter S0 Fraction Value:    .473
```

Figure A-3 shows Enter value in program

```

core(3) row(3)
Enter Pc Lab Value: 10
Enter Sw Fraction Value: .263
core(3) row(4)
Enter Pc Lab Value: 30
Enter Sw Fraction Value: .198
core(3) row(5)
Enter Pc Lab Value: 60
Enter Sw Fraction Value: .180
core(3) row(6)
Enter Pc Lab Value: 100
Enter Sw Fraction Value: .161
core(3) row(7)
Enter Pc Lab Value: 200
Enter Sw Fraction Value: .14
core(4) row(1)
Enter Pc Lab Value: 1
Enter Sw Fraction Value: .958
core(4) row(2)
Enter Pc Lab Value: 4
Enter Sw Fraction Value: .820
core(4) row(3)
Enter Pc Lab Value: 10
Enter Sw Fraction Value: .692
core(4) row(4)
Enter Pc Lab Value: 30
Enter Sw Fraction Value: .610
core(4) row(5)
Enter Pc Lab Value: 60
Enter Sw Fraction Value: .560
core(4) row(6)
Enter Pc Lab Value: 100
Enter Sw Fraction Value: .524
core(4) row(7)
Enter Pc Lab Value: 200
Enter Sw Fraction Value: .474

```

fx

Figure A-4 shows Enter values in program

Command Window

```
Enter Cos_R Value:   .866
Enter Cos_L Value:   1
Enter Tension_R Value:  30
Enter Tension_L Value:  72

      core(1)
Enter K Value:   4.71
Enter Prosimy Value:   .123

      core(2)
Enter K Value:   528
Enter Prosimy Value:   .184

      core(3)
Enter K Value:   2078
Enter Prosimy Value:   .235

      core(4)
Enter K Value:   1.83
Enter Prosimy Value:   .113

Enter po value:   64.1
Enter po value:   43.7
```

Figure A-5 shows Enter values in program

```

K_AV =
    55.7154

Pro_AV =
    0.1628

Swi_AV =
    0.2122

core    (1)      PC_R  table:
ans =    (2)      (3)      (4)

    0.2608      0.2608      0.2608      0.2608
    1.4433      1.4433      1.4433      1.4433
    2.6082      2.6082      2.6082      2.6082
   10.8250     10.8250     10.8250     10.8250
   21.6500     21.6500     21.6500     21.6500
   36.0832     36.0832     36.0832     36.0832
   72.1667     72.1667     72.1667     72.1667

```

Figure A-6 shows Results PC_R and Porosity avg. and permeability avg.

```

Command Window

core    (1)      PC_R  table:
ans =    (2)      (3)      (4)

    0.3611      0.3611      0.3611      0.3611
    1.4444      1.4444      1.4444      1.4444
    3.6111      3.6111      3.6111      3.6111
   10.8333     10.8333     10.8333     10.8333
   21.6667     21.6667     21.6667     21.6667
   36.1111     36.1111     36.1111     36.1111
   72.2222     72.2222     72.2222     72.2222

core    (1)      J_Func  table:
ans =    (2)      (3)      (4)

    0.0186      0.2025      0.2827      0.0121
    0.0744      0.8101      1.1308      0.0484
    0.1860      2.0252      2.8269      0.1210
    0.5581      6.0755      8.4808      0.3629
    1.1162     12.1510     16.9615      0.7259
    1.8603     20.2516     28.2692      1.2098
    3.7206     40.5032     56.5385      2.4196

```

Figure A-7 shows Results J-function.

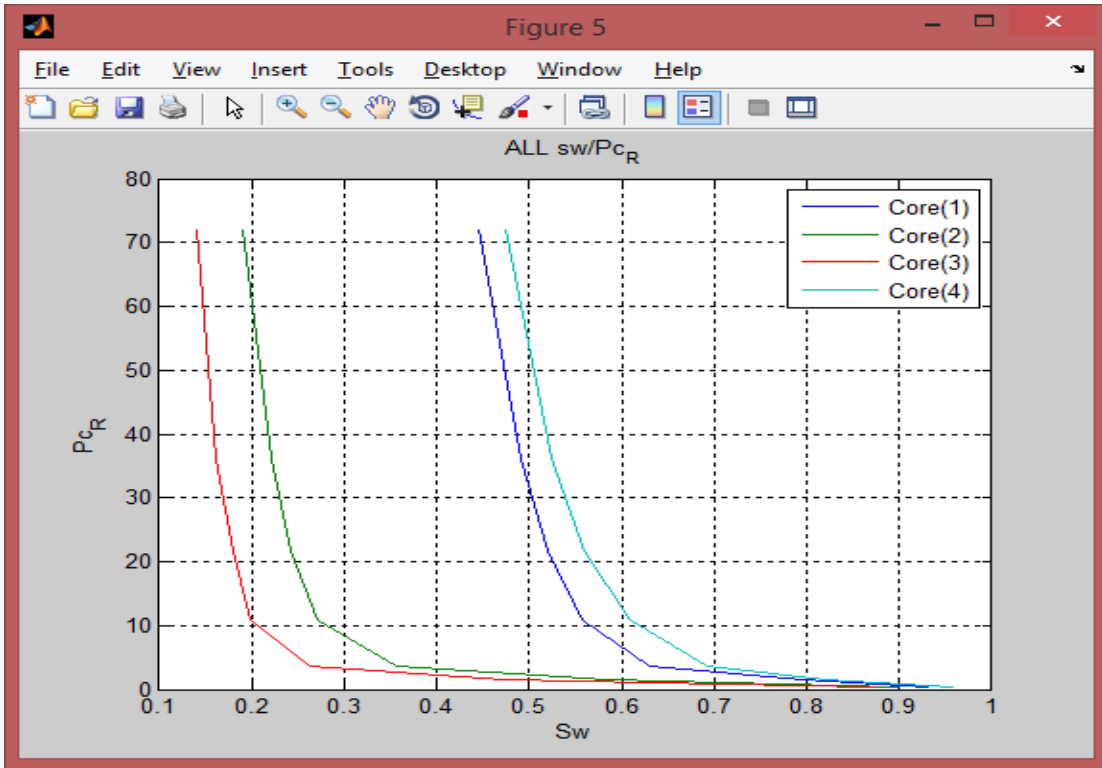


Figure A-8 shows relationship between Sw and Pc_R

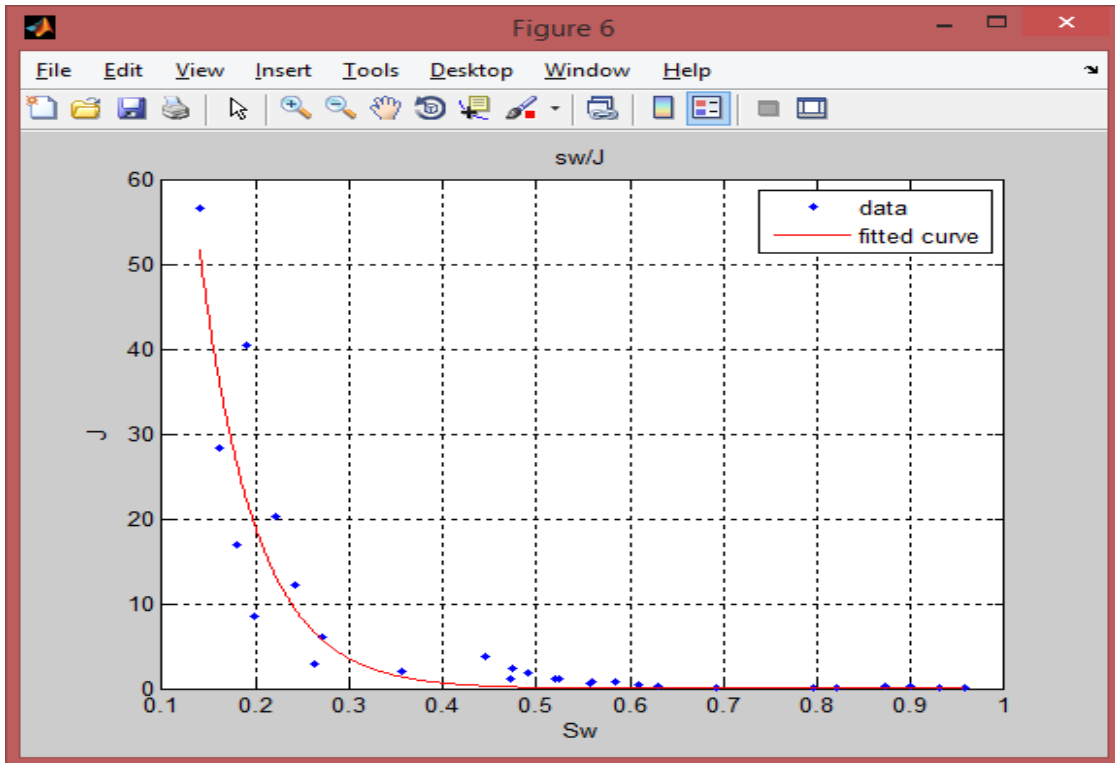


Figure A-9 shows relationship between Sw and J

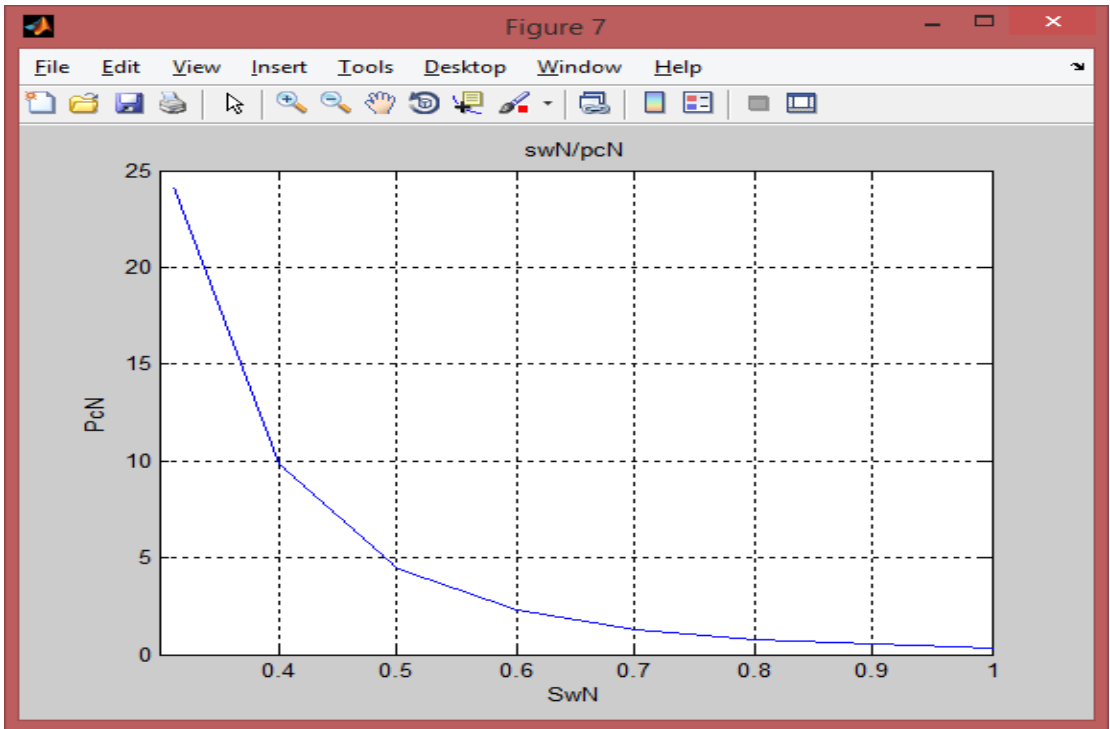


Figure A-10 shows relationship between SwN and PcN

```

Sw_New      Jnew      PcNew      hft      hm
All =
1.0000      0.0580      0.3575      2.5236      0.7694
0.9000      0.0849      0.5235      3.6954      1.1266
0.8000      0.1301      0.8019      5.6602      1.7257
0.7000      0.2109      1.3003      9.1783      2.7983
0.6000      0.3686      2.2718      16.0365      4.8892
0.5000      0.7131      4.3955      31.0274      9.4596
0.4000      1.5995      9.8589      69.5920      21.2171
0.3123      3.9204      24.1649      170.5758      52.0048

From Chart Sw_New/Pc_New Enter Pc value : 10

Tran_Zone =
68.0647

fx
>>
>>

```

Figure A-11 shows transition zone and all previously result


```

50 %vi_B0Prun/coreN
51
52 fprintf(' \n      PC table: \ncore ');
53 for s=1:N
54     fprintf(' (%.04) ',x);
55 end
56 Pr_B(1:row,L:N)
57
58 fprintf(' \n      V_Tune table: \ncore ');
59 for s=1:N
60     fprintf(' (%.04) ',x);
61 end
62 V(1:row,L:N)
63
64 for N=1:coreN;
65 for N=1:row;
66     sv(B,N)=core(B,L,N);
67 end
68 end
69
70 Fig1:
71
72 for N=1:coreN;
73 figure(Fig)
74 plot(sv(1:row,N),Pr_B(1:row,N));
75 grid on;
76 title(' sv/pc_B ');
77 xlabel(' \nu '); ylabel(' Pr_B ');
78 FigFig1;
79 end
80
81 figure(Fig)
82 plot(sv,Pr_B);
83 legend('Core(1)', 'Core(2)', 'Core(3)', 'Core(4)', 'Core(5)', 'Core(6)', 'Core(7)', 'Core(8)');
84 grid on;
85 title(' ALL sv/Pr_B ');
86 xlabel(' \nu '); ylabel(' Pr_B ');
87 FigFig1;
88
89 A = reshape(sv,[],L);
90 B = reshape(Pr,[],L);
91
92 figure(Fig)
93 f = fit(A, B, 'exp1 ');
94 plot(f,A,B);
95 grid on;
96 title(' sv/B ');
97 xlabel(' \nu '); ylabel(' P ');
98 FigFig1;

```

Figure A-12 shows the codes of used

```

1 coreN=input('Enter The Number Of Core: ');
2 row=input('Enter The Number Of row: ');
3 column=1;
4 for N=1:coreN;
5     for R=1:row;
6
7         fprintf('core(%d,%d) row(%d,%d)\n',N,R);
8         core(R,N)=input('Enter Pc Lab Value: ');
9         core(R,N)=input('Enter In Fraction Value: ');
10        end
11    end
12    fprintf('\n P<sub>L</sub> = P<sub>F</sub>');
13    core(L,row,L:column,1:coreN)
14
15    Cos_B=input('Enter Cos B Value: ');
16    Cos_L=input('Enter Cos L Value: ');
17    Tension_B=input('Enter Tension B Value: ');
18    Tension_L=input('Enter Tension L Value: ');
19
20    for N=1:coreN;
21        for R=1:row;
22            Pc_B(R,N)=core(R,L,N)*Cos_B*Tension_B/(Cos_L*Tension_L);
23        end
24    end
25
26    K_B=1;
27    Pro_B=0;
28    for N=1:coreN;
29        fprintf('\n core(%d,%d) \n',N);
30        K=input('Enter K Value: ');
31        Proximity=input('Enter Proximity Value: ');
32        K_B=K*B^PK;
33        Pro_B=Pro_B+Proximity;
34        for R=1:row;
35            f(R,N)=0.22645*Pc_B(R,N)^0.5*(K/Proximity)/(Cos_B*Tension_B);
36        end
37    end
38    fprintf('\n');
39
40    po=input('Enter po value: ');
41    po=input('Enter po value: ');
42
43    K_B=K_B*(L/coreN)
44    Pro_B=Pro_B/coreN
45
46    run=0;
47    for N=1:coreN;
48        run=run+core(row,L,N);
49    end

```

Figure A-13 shows the codes of used

```

97 xlabel('σ'); ylabel('ε');
98 FigFigure;
99
100 i=1; B=1;
101 while i>=0.1
102     σ(i,B)=i;
103     i=i+0.1;
104     B=B+1;
105     if Stri_B(i)
106         σ(i,B)=Stri_B(i);
107         break;
108     end
109 end
110
111 for B=1:B
112     Stri(B,i)=0.051*σ(i,B)^-0.02;
113 end
114
115 for B=1:B;
116     PctDev(B,i)=Stri(B,i)*Tension_B(i)*gpr(Pro_B(i)/X_B(i))/0.1166;
117 end
118
119 figure(Fig);
120 plot(σ, PctDev);
121 grid on;
122 title('σ vs PctDev');
123 xlabel('σ(MPa)'); ylabel('PctDev');
124 FigFigure;
125
126 for B=1:B;
127     Stri(B,i)=144*PctDev(B,i)/(gpr-po);
128 end
129
130 for B=1:B;
131     ln(B,i)=Stri(B,i)/0.28;
132 end
133
134 figure(Fig);
135 plot(σ, ln);
136 grid on;
137 title('σ vs ln');
138 xlabel('σ(MPa)'); ylabel('ln');
139 FigFigure;
140
141 fprintf('ln    Stri    Stri    PctDev    Stri    ln\n');
142 all=[σ    Stri    PctDev    Stri    ln];
143
144 Pct=fprintf('From Chart Stri Dev Center Pct value : ');
145 Tran_Zone=144*(Pct-PctDev(1,1))/(gpr-po)

```

Figure A-14 shows the codes of used

The codes of used

```
coreN=input('Enter The Number Of Core: ');
row=input('Enter The Number Of row: ');
column=2;
for N=1:coreN;
for R=1:row;

fprintf('core(%.0f) row(%.0f)\n',N,R);
core(R,1,N)=input('Enter Pc Lab Value: ');
core(R,2,N)=input('Enter Sw Fraction Value: ');
end
end
fprintf('\n PC_L Sw_F');
core(1:row,1:column,1:coreN)

Cos_R=input('Enter Cos_R Value: ');
Cos_L=input('Enter Cos_L Value: ');
Tension_R=input('Enter Tension_R Value: ');
Tension_L=input('Enter Tension_L Value: ');

for N=1:coreN;
for R=1:row;
Pc_R(R,N)=core(R,1,N)*Cos_R*Tension_R/(Cos_L*Tension_L);
end
end

K_AV=1;
Pro_AV=0;
for N=1:coreN;
fprintf('\n core(%.0f) \n',N);
K=input('Enter K Value: ');
Prosity=input('Enter Prosimy Value: ');
K_AV=K_AV*K;
Pro_AV=Pro_AV+Prosity;
for R=1:row;
J(R,N)=0.21645*Pc_R(R,N)*sqrt(K/Prosity)/(Cos_R*Tension_R);
end
end
fprintf('\n');
```

```

pw=input('Enter pw value: ');
po=input('Enter po value: ');

K_AV=K_AV^(1/coreN)
Pro_AV=Pro_AV/coreN

sum=0;
for N=1:coreN;
sum=sum+core(row,2,N);
end
Swi_AV=sum/coreN

fprintf('\n      PC_R table: \ncore ');
for x=1:N
fprintf(' (%.0f) ',x);
end
Pc_R(1:row,1:N)

fprintf('\n      J_Func table: \ncore ');
for x=1:N
fprintf(' (%.0f) ',x);
end
J(1:row,1:N)

for N=1:coreN;
for R=1:row;
sw(R,N)=core(R,2,N);
end
end

Fig=1;

for N=1:coreN;
figure(Fig)
plot(sw(1:row,N),Pc_R(1:row,N));
grid on;
title('sw/pc_R');
xlabel('Sw'); ylabel('Pc_R');
Fig=Fig+1;

```

```

end

figure(Fig)
plot(sw,Pc_R);
legend('Core(1)','Core(2)','Core(3)','Core(4)','Core(5)','Core(6)','Core(7)');
legend('Core(8)');
grid on;
title('ALL sw/Pc_R');
xlabel('Sw'); ylabel('Pc_R');
Fig=Fig+1;

A = reshape(sw,[],1);
B = reshape(J,[],1);

figure(Fig)
f = fit( A, B, 'exp1' );
plot(f,A,B);
grid on;
title('sw/J');
xlabel('Sw'); ylabel('J');
Fig=Fig+1;

i=1; R=1;
while i>=0.1
swN(R,1)=i;
i=i-0.1;
R=R+1;
if Swi_AV>i
swN(R,1)=Swi_AV;
break;
end
end

for N=1:R
Jnew(N,1)=0.058*swN(N,1)^-3.62;
end

for N=1:R;
PcNew(N,1)=Jnew(N,1)*Tension_R*Cos_R*sqrt(Pro_AV/K_AV)/0.
21645;

```

```

end

figure(Fig);
plot(swN,PcNew);
grid on;
title('swN/pcN');
xlabel('SwN'); ylabel('PcN');
Fig=Fig+1;

for N=1:R;
hft(N,1)=144*PcNew(N,1)/(pw-po);
end

for N=1:R;
hm(N,1)=hft(N,1)/3.28;
end

figure(Fig);
plot(swN,hm);
grid on;
title('swN/hm');
xlabel('SwN'); ylabel('hm');
Fig=Fig+1;

fprintf('\n Sw_New Jnew PcNew hft hm',x);
All=[swN Jnew PcNew hft hm]

Pc=input('From Chart Sw_New/Pc_New Enter Pc value : ');
Tran_Zone=144*(Pc-PcNew(1,1))/(pw-po)

fprintf('\nThis Program Was Designed In 2017 By Engineers:\n1)
ADAM HASSAN AL-ROUM.\n2) OTHMAN ABDULLAH AL-
QAISI.\n3) ABDULMOULA ADAM SALEH.\n4) MOHAMMED
MAHMOUD MOHAMMED.');
```